

This discussion paper is/has been under review for the journal Atmospheric Chemistry and Physics (ACP). Please refer to the corresponding final paper in ACP if available.

# Mesosphere-to-stratosphere descent of odd nitrogen in February–March 2009 after sudden stratospheric warming

S.-M. Salmi<sup>1,2</sup>, P. T. Verronen<sup>1</sup>, L. Thölix<sup>1</sup>, E. Kyrölä<sup>1</sup>, L. Backman<sup>1</sup>,  
A. Yu. Karpechko<sup>1</sup>, and A. Seppälä<sup>1,3</sup>

<sup>1</sup>Finnish Meteorological Institute, Helsinki, Finland

<sup>2</sup>Department of Physics, University of Helsinki, Helsinki, Finland

<sup>3</sup>British Antarctic Survey (NERC), Cambridge, UK

Received: 23 November 2010 – Accepted: 22 December 2010 – Published: 18 January 2011

Correspondence to: S.-M. Salmi (sanna-mari.salmi@fmi.fi)

Published by Copernicus Publications on behalf of the European Geosciences Union.

ACPD

11, 1429–1455, 2011

**Descent of odd  
nitrogen after sudden  
stratospheric  
warming**

S.-M. Salmi et al.

Title Page

Abstract

Introduction

Conclusions

References

Tables

Figures

⏪

⏩

◀

▶

Back

Close

Full Screen / Esc

Printer-friendly Version

Interactive Discussion

## Abstract

We use the 3-D FinROSE chemistry transport model (CTM) and ACE-FTS (Atmospheric Chemistry Experiment Fourier Transform Spectrometer) observations to study the connection between atmospheric dynamics and  $\text{NO}_x$  descent during early 2009 in the northern polar region. We force the model  $\text{NO}_x$  at 80 km poleward of  $60^\circ\text{N}$  with ACE-FTS observations and then compare the model results with observations at lower altitudes. Low geomagnetic indices indicate absence of local  $\text{NO}_x$  production in early 2009, which gives a good opportunity to study the effects of atmospheric transport on polar  $\text{NO}_x$ . No in-situ production of  $\text{NO}_x$  by energetic particle precipitation is therefore included. This is the first model study using ECMWF (The European Centre for Medium-Range Weather Forecasts) data up to 80 km and simulating the exceptional winter of 2009 with one of the strongest major sudden stratospheric warmings (SSW). The model results show a strong  $\text{NO}_x$  descent in February–March 2009 from the upper mesosphere to the stratosphere after the major SSW. Both observations and model results suggest an increase of  $\text{NO}_x$  to 150–200 ppb (i.e. by factor of 50) at 65 km due to the descent following the SSW. The model, however, underestimates the amount of  $\text{NO}_x$  around 55 km by 40–60 ppb. The results also show that the chemical loss of  $\text{NO}_x$  was insignificant i.e.  $\text{NO}_x$  was mainly controlled by the dynamics. Both ACE-FTS observations and FinROSE show a decrease of ozone of 20–30% at 30–50 km after mid-February to mid-March. However, these changes are not related to the  $\text{NO}_x$  descent, but are due to activation of the halogen chemistry.

## 1 Introduction

In the stratosphere odd nitrogen ( $\text{NO}_x = \text{NO} + \text{NO}_2$ ) is produced mainly by oxidation of nitrous oxide ( $\text{N}_2\text{O}$ ). Significant production occurs also in the lower thermosphere, around 110 km, through photoionization of  $\text{N}_2$  by extreme ultraviolet (EUV) and soft X-ray radiation. In the polar regions, another important although highly varying source

ACPD

11, 1429–1455, 2011

## Descent of odd nitrogen after sudden stratospheric warming

S.-M. Salmi et al.

Title Page

Abstract

Introduction

Conclusions

References

Tables

Figures

⏪

⏩

◀

▶

Back

Close

Full Screen / Esc

Printer-friendly Version

Interactive Discussion



of  $\text{NO}_x$  is ionizing energetic particle precipitation directly affecting the wide range of altitudes from the thermosphere down to the stratosphere (Barth, 1992; Vitt et al., 2000). Because  $\text{NO}_x$  loss is driven by photodissociation, in the absence of solar radiation  $\text{NO}_x$  is chemically long-lived and therefore strongly affected by atmospheric dynamics. It has been suggested that  $\text{NO}_x$  transport could provide a connection mechanism between particle precipitation in the mesosphere-lower thermosphere (MLT) and stratospheric ozone (Solomon et al., 1982; Siskind et al., 1997; Callis and Lambert, 1998). Further, possible influence of particle precipitation and ozone changes to regional ground-level climate has been discussed although the linking mechanisms are not yet understood (Rozanov et al., 2005; Seppälä et al., 2009). In the recent years, observations have shown that during winter times  $\text{NO}_x$  can be effectively transported downwards inside the polar vortex (Funke et al., 2005; Hauchecorne et al., 2007; Seppälä et al., 2007; Randall et al., 2009). This has typically been more pronounced in the Northern Hemisphere where the exceptionally strong descent events have been related to reformation of the vortex following its split/displacement due to sudden stratospheric warming events, e.g. in 2004, 2006, and 2009 (Randall et al., 2009; Manney et al., 2009). Although the satellite observations of  $\text{NO}_x$  often cover altitudes up to middle mesosphere only, the connection to lower thermospheric  $\text{NO}_x$  production has been established using VLF radio data in the case of the 2004 descent (Clilverd et al., 2006).

Previous modelling studies have already addressed the importance of wintertime  $\text{NO}_x$  enhancements to middle atmospheric composition. Vogel et al. (2008) studied the effects of descending  $\text{NO}_x$  on ozone during the Arctic winter 2003–2004. The results indicate a decrease of ozone between 3.3 and 18.0 Dobson units (DU) and are in good agreement with MIPAS (Michelson Interferometer for Passive Atmospheric Sounding) and ACE-FTS observations. Compared to the observations, the amount of  $\text{NO}_x$  was however underestimated by the model at 45–50 km. Baumgaertner et al. (2009) studied the production of  $\text{NO}_x$  due to low energy electrons. The model results underestimated the amount of  $\text{NO}_x$  by about 5 ppb at 55 km altitude during a strong enhancement period of  $\text{NO}_x$  in the Northern Hemisphere, but the model still captured

## Descent of odd nitrogen after sudden stratospheric warming

S.-M. Salmi et al.

[Title Page](#)[Abstract](#)[Introduction](#)[Conclusions](#)[References](#)[Tables](#)[Figures](#)[⏪](#)[⏩](#)[◀](#)[▶](#)[Back](#)[Close](#)[Full Screen / Esc](#)[Printer-friendly Version](#)[Interactive Discussion](#)

the main features observed by MIPAS. Reddmann et al. (2010) continued the work of Vogel et al. (2008) by covering years 2002–2004 and considering stratospheric chemistry in more detail. They estimated that in total 5.4 giga moles of  $\text{NO}_y$  descended into the stratosphere, while the total ozone column was reduced by several DU. Both  $\text{NO}_x$  and ozone concentrations were underestimated around 45 km altitude. The underestimation of ozone was attributed to missing transport from mid to high latitudes.

One of the strongest major SSWs on record occurred in the Northern Hemisphere in January 2009 (Manney et al., 2009). According to observations of the Microwave Limb Sounder (MLS), the stratopause broke down in late January and then reformed at very high altitudes around 80 km. During the major SSW the polar vortex split, but reformed after the SSW in the upper stratosphere where it became stronger than it initially was. Randall et al. (2009) used ACE-FTS data and showed that following the SSW stratospheric  $\text{NO}_x$  increased due to strong downward transport by factor of approximately 50 compared to winters without descent events. The results indicated that  $\text{NO}_x$  enhancement in 2009 was due to the unusual meteorology rather than geomagnetic activity, which at the time was lower than average. No significant effect on ozone was reported.

In this paper we analyse the dynamics and meteorology of the unusual winter of 2009 in the northern polar region using ECMWF operational analyses. Extending the work of Randall et al. (2009), we use the FinROSE chemistry transport model (CTM) to first time simulate the exceptional winter of 2009. This is done by constraining the model  $\text{NO}_x$  by enforcing a time-dependent upper boundary condition (UBC) based on ACE-FTS observations between 75 and 85 km altitude. Compared to earlier studies (e.g. Vogel et al., 2008; Reddmann et al., 2010), in this study the model uses ECMWF operational analyses for dynamics up to 80 km, which gives us the opportunity to study the  $\text{NO}_x$  descent starting as high as from the upper mesosphere. At the same time we can test the quality of ECMWF operational analyses at higher altitudes. For comparison, we simulate also the winter of 2007, which was completely different compared to 2009 and did not include any extreme meteorological events.

## Descent of odd nitrogen after sudden stratospheric warming

S.-M. Salmi et al.

[Title Page](#)[Abstract](#)[Introduction](#)[Conclusions](#)[References](#)[Tables](#)[Figures](#)[⏪](#)[⏩](#)[◀](#)[▶](#)[Back](#)[Close](#)[Full Screen / Esc](#)[Printer-friendly Version](#)[Interactive Discussion](#)

## 2 Model and measurements

### 2.1 Chemistry transport model FinROSE

FinROSE is a global 3-dimensional CTM designed for middle atmospheric studies (Damski et al., 2007). The model dynamics (i.e. temperature, horizontal winds and pressure) are from external sources i.e. changes in atmospheric composition do not affect the modelled dynamics. Vertical wind is calculated inside the model by using the continuity equation. In this study FinROSE has 41 vertical levels (0–80 km), a horizontal resolution of  $10^{\circ} \times 5^{\circ}$  and is driven by operational analyses from ECMWF. The resolutions and the number of vertical levels can be modified depending on the resolution of the meteorological data. FinROSE produces distributions of 40 species and families, but transport is applied only to the long-lived compounds. The model includes about 120 homogeneous reactions and 30 photodissociation processes. Chemical kinetic data, reaction rate coefficients and absorption cross-sections are taken from look-up-tables based on the Jet Propulsion Laboratory compilation by Sander et al. (2006). Photodissociation frequencies are calculated using a radiative transfer model (Kylling et al., 1997). In addition to homogeneous chemistry, the model also includes heterogeneous chemistry, i.e. formation and sedimentation of PSCs and reactions on PSCs. Chemistry is not defined in the troposphere, but the tropospheric abundances are given as boundary conditions. At the lower boundary, monthly averages from ECMWF are used for ozone and water vapour. Methane, instead, is relaxed towards climatological values and long-lived trace gases towards long time trends.

The ECMWF operational analyses are based on simulations of a general circulation model (GCM) using four dimensional data assimilation (4D-VAR). Horizontal resolution of the analyses used in this study is interpolated to a  $10^{\circ} \times 5^{\circ}$  (longitude  $\times$  latitude) grid and the number of vertical levels equals to 91 so that the upmost level is at 0.01 hPa (80 km). It has, however, been suggested by Manney et al. (2008) that the analyses are not consistent with observations above about 50 km because of the non-existent constraint by observational data and the inclusion of a only simplified parametrization

## Descent of odd nitrogen after sudden stratospheric warming

S.-M. Salmi et al.

Title Page

Abstract

Introduction

Conclusions

References

Tables

Figures

⏪

⏩

◀

▶

Back

Close

Full Screen / Esc

Printer-friendly Version

Interactive Discussion



of non-orographic gravity wave drag to the GCM. Moreover, the model top at 80 km is near the highest level of the stratopause observed e.g. during the major SSW in 2009. According to Manney et al. (2008) these deficiencies lead to the failure of the analyses to capture the stratopause variations during extreme meteorological conditions.

5 The operational analyses agree, however, well with satellite observations of MLS and SABER (Sounding of the Atmosphere using Broadband Emission Radiometry) in early winter stratopause temperatures. Because the ECMWF operational analyses have been used in the FinROSE-CTM up to 80 km, all the issues mentioned above might influence the model results.

## 10 2.2 Observations

We have used observations from the FTS (Fourier Transform Spectrometer) instrument onboard the ACE satellite (Atmospheric Chemistry Experiment) (Bernath et al., 2005). ACE-FTS is a solar occultation instrument launched in 2003. The instrument operates in the wavelength region of 2.2–13.3  $\mu\text{m}$  and measures vertical profiles of temperature, pressure, density and 18 atmospheric molecules in the altitude range of 15 10–150 km. Figure 1 shows the daily medians of the measurement locations north of 60° N in January–March 2007 and 2009. The median is calculated only, when there are at least five measurements available during a day. Otherwise the measurements for that particular day are neglected. The figure shows that the measurements represent almost the same latitudes from year to year. Measuring error for  $\text{NO}_x$  depends on altitude and concentration (not shown) so that at 80 km altitude the error is 1–3% for mixing ratios such as in late February–early March in 2009 and increases up to 20 10–15% for  $\text{NO}_x$  amounts observed in January 2009.

In this study we use ACE-FTS observations of  $\text{NO}_x$  as an UBC for FinROSE (Fig. 1), which is in effect on latitudes poleward of 60° N. We calculated two-day means from the observations for both 2007 and 2009 and used them at the upper boundary. In case of missing data we 1) assume one day's value as the two-day mean 2) if both 25 days are missing, use the previous two-day mean. However, the instrument changed

## Descent of odd nitrogen after sudden stratospheric warming

S.-M. Salmi et al.

Title Page

Abstract

Introduction

Conclusions

References

Tables

Figures



Back

Close

Full Screen / Esc

Printer-friendly Version

Interactive Discussion



**Descent of odd nitrogen after sudden stratospheric warming**

S.-M. Salmi et al.

[Title Page](#)[Abstract](#)[Introduction](#)[Conclusions](#)[References](#)[Tables](#)[Figures](#)[⏪](#)[⏩](#)[◀](#)[▶](#)[Back](#)[Close](#)[Full Screen / Esc](#)[Printer-friendly Version](#)[Interactive Discussion](#)

the direction of the measurements towards lower latitudes after 5 February, which can be seen as a decrease of about 400 ppb in the 2009 NO<sub>x</sub> mixing ratios (Fig. 1). Around 16 February ACE-FTS continued measuring on northern latitudes (>60° N) and NO<sub>x</sub> concentrations increased because of this. The effect can be seen as a minimum in the 2009 NO<sub>x</sub> mixing ratios between 10 and 28 February in Fig. 1. This means that the ACE-FTS measurements do not give a representative general view of the situation in the polar region during this time period. To reduce the influence of the change in the measuring direction, we replaced the 2009 ACE-FTS observations with interpolated values over the minimum (blue circles in Fig. 1) and neglected the largest values. This is somewhat arbitrary, but perhaps the best approach taking into account the lack of usable data in this time period.

### 3 Results

#### 3.1 Meteorological conditions

Figure 2 shows zonal mean temperature at 75° N for 2007 and 2009 as a function of time and altitude. The winter of 2007 was rather stable and no major stratopause break downs occurred. However, the temperatures increased around 24 February below 35 km, which can be seen as a drop of warm air from the stratopause to lower altitudes. The situation in 2009 was completely different as the stratopause warmed and dropped below 30 km in late January. This warming was accompanied by a descent of isentrops (i.e. isolines of potential temperature) while the concurrent cooling above 50 km was accompanied by an ascend of isentrops (not shown), indicating that these temperature changes were adiabatic. The descended isentrops relaxed upwards after the warming. The stratopause reformed after the break down around 80 km in early February, which led to very low temperatures between 30 and 50 km. The stratopause reformation seen in Fig. 2 is quite moderate compared to MLS observations shown by Manney

et al. (2009). This is probably due to the deficiencies in the ECMWF GCM already discussed in Sect. 2.1. Discontinuation in the temperature data on 10 March in 2009 is due to changes in the ECMWF operational model.

During the northern polar winter the direction of the zonal flow in the stratosphere is westerly (positive) and enables thus the vertical propagation of planetary waves from troposphere to stratosphere (Holton, 2004). Planetary wave amplification in the stratosphere decelerates the zonal wind and the polar jet, which leads to warming of the polar stratosphere. In case of a major SSW, the zonal mean wind changes direction from westerly to easterly (negative) and thus prevents the vertical propagation of planetary waves. Figure 3 shows the zonal mean winds in 2007 and 2009 for latitude 75° N. Although there was no large increase in temperatures in 2007, the reversal of the zonal wind is clear. The changes in the wind direction and speed lasted only about 10 days, in contrast to the situation in 2009, when the easterly winds persisted until early March. This one month period of easterly winds in 2009 led to a low wave activity above the critical level, which for stationary waves corresponds to a level where the zonal wind speed equals to zero, and enabled the formation of a strong polar vortex, which broke up not until early March.

According to McInturff (1978), the criteria for a major SSW are fulfilled when the latitudinal mean temperature at 10 hPa ( $\approx 30$  km) or below increases poleward of 60° N and the zonal winds are reversed from westerly to easterly in the same area. Figure 4 shows the zonal mean temperature at 10 hPa as a function of time and latitude. The poleward temperature gradient reversed during both winters. In 2007 the gradient was fairly small ( $\approx 10$  K northward of 60° N) and lasted about 10 days. The warming in 2009 was more pronounced and the temperature gradient was positive for approximately 20 consecutive days in the polar region. The zonal mean wind at 10 hPa (Fig. 5) reversed from westerly to easterly at the same time when the poleward temperature gradient became positive in 2007 and 2009. This indicates that a major SSW occurred in both winters. However, the situation in 2007 returned to undisturbed winter conditions in a few days, which is more common for minor SSWs. In addition, the easterly phase of

## Descent of odd nitrogen after sudden stratospheric warming

S.-M. Salmi et al.

[Title Page](#)[Abstract](#)[Introduction](#)[Conclusions](#)[References](#)[Tables](#)[Figures](#)[⏪](#)[⏩](#)[◀](#)[▶](#)[Back](#)[Close](#)[Full Screen / Esc](#)[Printer-friendly Version](#)[Interactive Discussion](#)

the zonal mean winds blocked the vertical propagation of planetary waves only for such a short period of time that the polar vortex in the upper stratosphere/lower mesosphere did not have time to recover. In 2009 the wind reversal to westerly took about one month, giving enough time for the vortex to recover in the upper stratosphere/lower mesosphere. The criteria for a major SSW in 2009 were first met on the 24th of January (black vertical dashed line in Figs. 4 and 5).

### 3.2 NO<sub>x</sub> descent

Figure 6 presents NO<sub>x</sub> observations measured by ACE-FTS in 2007 (top) and 2009 (bottom). Plotted are daily medians north of 60° N, which correspond to measurement locations shown in Fig. 1. Observations show that there were large differences in the distribution of NO<sub>x</sub> between years 2007 and 2009. In 2007 the mesospheric maximum of NO<sub>x</sub> reached 60–65 km in the beginning of the year and then ascended towards the spring. This can be explained by changes in the zonal mean temperature and wind fields (Figs. 2 and 3). The stratopause was quite stable until the beginning of February, when the temperatures increased for a few days and the westerly winds weakened. Warm midlatitude air with low NO<sub>x</sub> concentrations mixed with the colder polar air and decreased the NO<sub>x</sub> concentrations. This warming did not dislocate the stratopause and the temperatures remained quite high even after the warming. The warming in late February produced no significant effects on NO<sub>x</sub>.

The major SSW in 2009, instead, had a great impact on NO<sub>x</sub>. A tongue-like structure of descending NO<sub>x</sub> from the mesosphere to the stratosphere after the SSW is clearly seen in Fig. 6. High NO<sub>x</sub> amounts were transported from 80 to 55 km altitude in about 40 days. The descent took place during the recovery of the polar vortex and is also discussed by Randall et al. (2009). The fact that the NO<sub>x</sub> concentration isolines crossed the isentrops (not shown) suggests that the descent was diabatic, consistent with the analysis by Manney et al. (2008) of a similar upper stratospheric vortex recovery after the SSW during winter 2005/2006. After early March the descent stopped and NO<sub>x</sub> concentrations normalized quickly. At this time the stratopause had already reformed

## Descent of odd nitrogen after sudden stratospheric warming

S.-M. Salmi et al.

Title Page

Abstract

Introduction

Conclusions

References

Tables

Figures

⏪

⏩

◀

▶

Back

Close

Full Screen / Esc

Printer-friendly Version

Interactive Discussion



and the zonal winds had started to reverse back to westerly (Fig. 3) allowing planetary waves to propagate upward, interact with the vortex, and mix the low-NO<sub>x</sub> air from outside the vortex with high-NO<sub>x</sub> air inside the vortex.

Figure 7 shows NO<sub>x</sub> timeseries calculated from FinROSE-CTM results. The data are daily means, calculated using only the grid points corresponding to ACE-FTS measurement locations (Fig. 1). The model reproduces the distribution of NO<sub>x</sub> reasonably well compared to the observations shown in Fig. 6. The maximum of NO<sub>x</sub> in the beginning of 2007 at about 75 km is of the same order of magnitude (800–900 ppb) as in the observations, but extends 3–5 km lower in the middle atmosphere. In 2009 the observations and model results show an increase of NO<sub>x</sub> to 150–200 ppb at 65 km. The modelled and observed NO<sub>x</sub> both descend to about 55 km altitude, but the amount of NO<sub>x</sub> is underestimated in the model by 40–60 ppb. The descent also starts 3–5 days earlier and lasts 3–5 days longer in the model than observed. Averaging the model results over the whole polar cap (60° N–90° N) had only a slight effect on the model results (not shown). Compared to the sampled results (Fig. 7) the descent stopped a couple of days earlier above 60 km, but continued longer until late March between 50 and 60 km.

Figure 8 shows the model results and ACE-FTS observations at 80, 68 and 54 km altitudes. Differences at 80 km altitude during 10–28 February are due to the interpolated UBC at that time. However, the modified UBC improves the agreement between the model and observations at lower altitudes. There is a reasonable agreement between the model and the observations at 68 km altitude. An overestimation of about 100 ppb occurs after the 8 March, consistent with the fact that the descent lasted longer in the model than observed by ACE-FTS. Significant differences are found at 54 km where the model produces 40–60 ppb smaller values than found in the observations. The observed maximum of NO<sub>x</sub> occurs also about 10 days earlier compared to the model results. Overall, the model succeeds to reproduce the descent of NO<sub>x</sub>, with no in-situ production included in the model, reasonably well compared to the observations and confirms the results of Randall et al. (2009) about the importance of dynamics on the

## Descent of odd nitrogen after sudden stratospheric warming

S.-M. Salmi et al.

Title Page

Abstract

Introduction

Conclusions

References

Tables

Figures

⏪

⏩

◀

▶

Back

Close

Full Screen / Esc

Printer-friendly Version

Interactive Discussion

distribution of  $\text{NO}_x$ .

Distribution of  $\text{NO}_x$  calculated from the model results in the northern polar region ( $50^\circ\text{N}$ – $90^\circ\text{N}$ ) is illustrated in Fig. 9. The figure shows that descending  $\text{NO}_x$  reaches 69 km altitude already on 6 February with amounts of 80–100 ppb. The circular structure of  $\text{NO}_x$  in the polar region is due to the existing or evolving polar vortex. The effect of photochemistry can be considered negligible during the polar winter on latitudes poleward of  $60^\circ\text{N}$ . As in Fig. 8, in time  $\text{NO}_x$  can be found at constantly lower altitudes with mixing ratios of 60–80 ppb finally reaching 54 km on 15 March. ACE-FTS measurement locations are marked in the figure with filled white circles. It stands out that there are only about 10 measurements per day to observe the northern polar area. When the possible outliers are removed, even fewer observations are left to represent the whole polar cap region. This might lead to differences between observations and the model results, especially close to the polar vortex edge. In addition, the closest model grid to ACE-FTS measurement covers by definition a larger area ( $10^\circ \times 5^\circ$ ) than the point-form observation does and can also be inside the vortex, although the measurement was done outside the vortex. This can partly explain the differences between the model and observations.

To estimate the effect of chemistry on descending  $\text{NO}_x$ , we have added a  $\text{NO}_x$  tracer into the model. This means that the tracer uses the same boundary condition as  $\text{NO}_x$ , but no chemistry is done to the tracer. Transport is thus the only factor that affects the tracer. The relative effect of chemistry can be calculated by dividing the difference between  $\text{NO}_x$  and the tracer with the amount of  $\text{NO}_x$ . The model results indicate that the chemical production of  $\text{NO}_x$  is not effective during polar winter and, furthermore, the relative chemical loss is only 3% or less (not shown), meaning that chemistry does not have a significant effect on  $\text{NO}_x$  concentrations during the dark winter. Therefore  $\text{NO}_x$  can descend inside the arctic vortex with only little interference by chemistry. In addition to gas phase chemistry, also photodissociation processes affect the amount of  $\text{NO}_x$  in the middle and upper atmosphere. The time period from January to March in the northern polar area is very dark leading to only weak photodissociation processes and

**Descent of odd nitrogen after sudden stratospheric warming**

S.-M. Salmi et al.

Title Page

Abstract

Introduction

Conclusions

References

Tables

Figures



Back

Close

Full Screen / Esc

Printer-friendly Version

Interactive Discussion



thus to longer photochemical lifetimes. The winter of 2009 was not an exception and the photochemical lifetime of  $\text{NO}_x$  was nearly two months in early January decreasing to about 5 days towards the end of March in the altitude range of 60–80 km. This is a further evidence that  $\text{NO}_x$  was mainly influenced by atmospheric dynamics during the time period under investigation.

### 3.3 Effects on $\text{O}_3$

Both ACE-FTS and FinROSE-CTM show ozone decrease after mid-February starting from around 50 km (Fig. 10). The observations indicate ozone decrease of about 20% between 30–50 km lasting one month and recovery in early March. In the model, ozone depletion is about 30% i.e. stronger than observed while the recovery takes place later in mid-March. In addition, the model results show lower ozone mixing ratios around 40 km from mid-January to mid-February. However, ACE-FTS observations and model results show similar increases in ozone in late March at around 45 km.

The ozone decrease between late February and mid-March is not directly linked to the descent of  $\text{NO}_x$ . In fact, according to ACE-FTS observations  $\text{NO}_x$  did not descend below 50 km altitude and therefore can not explain the observed effect on ozone. The descent was somewhat stronger in the model compared to the observations, which led to small  $\text{NO}_x$  enhancements also below 50 km. The increase in  $\text{NO}_x$  concentrations at 40 km was, however, too small to alone have such an effect on ozone.

The dynamics could lead to ozone decrease at 40 km through transport of low ozone concentrations from above. Analysing the  $\text{O}_x$  tracer in the model, similarly to the  $\text{NO}_x$  tracer earlier, we find that ozone transport can not explain its decrease (not shown). The results were comparable to those of  $\text{NO}_x$  meaning that the descent stopped to about 50 km. Below 50 km the downward transport was too weak to explain the observed structure of ozone. In contrast, the behaviour of ozone below 50 km from the beginning of the year until mid-February, including ozone decrease in late January and early February, was largely determined by the dynamics. Differences between the observations and model results during the first month can at least partially be explained

## Descent of odd nitrogen after sudden stratospheric warming

S.-M. Salmi et al.

Title Page

Abstract

Introduction

Conclusions

References

Tables

Figures

⏪

⏩

◀

▶

Back

Close

Full Screen / Esc

Printer-friendly Version

Interactive Discussion



by the non-perfect correspondence of the closest model grid point with the daily median of the observations.

In the model, ozone destroying substances, such as bromine and chlorine, were produced after mid-February as the solar radiation increased and the chemical processes, including photodissociation, started to play an important role on atmospheric composition. These substances, with the help of a strong polar vortex, enabled the catalytic cycles destroying ozone and caused the observed depletion at 40 km. Later in March, as the solar radiation increased, ozone production began to dominate. As seen in Fig. 10, this led to increase of ozone in early March at 45 km altitude and then gradually also at lower altitudes.

## 4 Conclusions

ACE-FTS observations of  $\text{NO}_x$  show a strong descent event in the northern polar region in February–early March 2009 after the major SSW. Analysis of ECMWF wind and temperature data indicates that the reason behind the descent is the formation of a strong polar vortex in the upper stratosphere facilitated by the easterly zonal winds in the lower stratosphere, which prevented the vertical propagation of planetary waves. The descent of  $\text{NO}_x$  ended when the vortex weakened in early March. In contrast, the major SSW in late February 2007 was not as dramatic as that in January 2009. The changes in the winds and temperatures lasted only for about 10 days compared to approximately 20 days in 2009 and were not followed by  $\text{NO}_x$  descent.

We used FinROSE-CTM to simulate the 2009 descent of  $\text{NO}_x$  from the upper mesosphere to the stratosphere. The simulation were done by enforcing an upper boundary condition based on ACE-FTS observations of  $\text{NO}_x$ . This model study is the first one using ECMWF operational winds, temperature and pressure up to 80 km and the first model simulation of the exceptional winter of 2009.

The model results show a strong  $\text{NO}_x$  descent of about 700 m/day from mesosphere to stratosphere in February and early March 2009. Compared to the satellite observa-

### Descent of odd nitrogen after sudden stratospheric warming

S.-M. Salmi et al.

Title Page

Abstract

Introduction

Conclusions

References

Tables

Figures



Back

Close

Full Screen / Esc

Printer-friendly Version

Interactive Discussion



tions, the amount of  $\text{NO}_x$  is underestimated in the model at around 55 km by 40–60 ppb. Between 60 and 80 km the model results are in reasonable agreement with ACE-FTS observations. This agreement gives some confidence in the ECMWF operational analyses also above 50 km.

ACE-FTS observations showed a decrease in ozone of about 20% between 30–50 km coinciding with the 2009  $\text{NO}_x$  descent. However,  $\text{NO}_x$  did not descend below 50 km and does not explain the observed decrease of ozone. According to the FinROSE-CTM results, the reason behind the ozone decrease was the increasing amount of solar radiation that activated chlorine and bromine compounds which then catalytically destroyed ozone. In early March the solar radiation was already strong enough for ozone production, which led to increase of the ozone concentrations.

This study demonstrates the large yearly variations in the dynamical fields and the importance of these factors to the behavior of  $\text{NO}_x$ . The chemical processes affecting  $\text{NO}_x$  during the dark polar winter were found to be insignificant. Therefore our reasonably successful modeling of  $\text{NO}_x$  descent using ECMWF meteorological data and an UBC based on ACE-FTS observations of  $\text{NO}_x$  is further confirmation of the dominant role of dynamics in understanding these descent events.

*Acknowledgements.* S.-M. Salmi would like to thank Viktoria Sofieva for helpful comments. All the authors thank also Cora Randall, Lynn Harvey and Kaley Walker for their help with the ACE-FTS data. Funding from the Academy of Finland through the THERMES, SPOC, SAARA and MIDAT projects is gratefully acknowledged. A. Seppälä was supported by the European Commission project FP7-PEOPLE-IEF-2008/237461. The Atmospheric Chemistry Experiment (ACE) data were provided by the European Space Agency (ESA). ACE is a Canadian-led mission mainly supported by the Canadian Space Agency and the Natural Sciences and Engineering Research Council of Canada.

## Descent of odd nitrogen after sudden stratospheric warming

S.-M. Salmi et al.

Title Page

Abstract

Introduction

Conclusions

References

Tables

Figures

⏪

⏩

◀

▶

Back

Close

Full Screen / Esc

Printer-friendly Version

Interactive Discussion



## References

- Barth, C. A.: Nitric oxide in the lower thermosphere, *Planet. Space Sci.*, 40, 315–336, 1992. 1431
- Baumgaertner, A. J. G., Jöckel, P., and Brühl, C.: Energetic particle precipitation in ECHAM5/MESSy1 – Part 1: Downward transport of upper atmospheric NO<sub>x</sub> produced by low energy electrons, *Atmos. Chem. Phys.*, 9, 2729–2740, doi:10.5194/acp-9-2729-2009, 2009. 1431
- Bernath, P. F., McElroy, C. T., Abrams, M. C., Boone, C. D., Butler, M., Camy-Peyret, C., Carleer, M., Clerbaux, C., Coheur, P.-F., Colin, R., DeCola, P., DeMazière, M., Drummond, J. R., Dufour, D., Evans, W. F. J., Fast, H., Fussen, D., Gilbert, K., Jennings, D. E., Llewellyn, E. J., Lowe, R. P., Mahieu, E., McConnell, J. C., McHugh, M., McLeod, S. D., Michaud, R., Midwinter, C., Nassar, R., Nichitiu, F., Nowlan, C., Rinsland, C. P., Rochon, Y. J., Rowlands, N., Semeniuk, K., Simon, P., Skelton, R., Sloan, J. J., Soucy, M.-A., Strong, K., Tremblay, P., Turnbull, D., Walker, K. A., Walkty, I., Wardle, D. A., Wehrle, V., Zander, R., and Zou, J.: Atmospheric Chemistry Experiment (ACE): Mission overview, *Geophys. Res. Lett.*, 32, L15S01, doi:10.1029/2005GL022386, 2005. 1434
- Callis, L. B. and Lambeth, J. D.: NO<sub>y</sub> formed by precipitating electron events in 1991 and 1992: descent into the stratosphere as observed by ISAMS, *Geophys. Res. Lett.*, 25, 1875–1878, doi:10.1029/98GL01219, 1998. 1431
- Clilverd, M. A., Seppälä, A., Rodger, C. J., Verronen, P. T., and Thomson, N. R.: Ionospheric evidence of thermosphere-to-stratosphere descent of polar NO<sub>x</sub>, *Geophys. Res. Lett.*, 33, L19811, doi:10.1029/2006GL026727, 2006. 1431
- Damski, J., Thölix, L., Backman, L., Taalas, P., and Kulmala, M.: FinROSE – middle atmospheric chemistry transport model, *Boreal Environ. Res.*, 12, 535–550, 2007. 1433
- Funke, B., Lopéz-Puertas, M., Gil-López, S., von Clarmann, T., Stiller, G. P., Fischer, H., and Kellmann, S.: Downward transport of upper atmospheric NO<sub>x</sub> into the polar stratosphere and lower mesosphere during the Antarctic 2003 and Arctic 2002/2003 winters, *J. Geophys. Res.*, 110, D24308, doi:10.1029/2005JD006463, 2005. 1431
- Hauchecorne, A., Bertaux, J.-L., Dalaudier, F., Russell III, J. M., Mlynczak, M. G., Kyrölä, E., and Fussen, D.: Large increase of NO<sub>2</sub> in the north polar mesosphere in January–February 2004: evidence of a dynamical origin from GOMOS/ENVISAT and SABER/TIMED data, *Geophys. Res. Lett.*, 34, L03810, doi:10.1029/2006GL027628, 2007. 1431
- Holton, J. R.: *An Introduction to Dynamic Meteorology*, 4th edition, Elsevier academic press,

### Descent of odd nitrogen after sudden stratospheric warming

S.-M. Salmi et al.

Title Page

Abstract

Introduction

Conclusions

References

Tables

Figures

◀

▶

◀

▶

Back

Close

Full Screen / Esc

Printer-friendly Version

Interactive Discussion



## Descent of odd nitrogen after sudden stratospheric warming

S.-M. Salmi et al.

Title Page

Abstract

Introduction

Conclusions

References

Tables

Figures

⏪

⏩

◀

▶

Back

Close

Full Screen / Esc

Printer-friendly Version

Interactive Discussion

San Diego, California, USA, 2004. 1436

Kylling, A., Albold, A., and Seckmeyer, G.: Transmittance of a cloud is wavelength – dependent in the UV-range: physical interpretation, *Geophys. Res. Lett.*, 24(4), 397–400, doi:10.1029/97GL00111, 1997. 1433

5 Manney, G. L., Daffer, W. H., Strawbridge, K. B., Walker, K. A., Boone, C. D., Bernath, P. F., Kerzenmacher, T., Schwartz, M. J., Strong, K., Sica, R. J., Krüger, K., Pumphrey, H. C., Lambert, A., Santee, M. L., Livesey, N. J., Remsberg, E. E., Mlynczak, M. G., and Russell III, J. R.: The high Arctic in extreme winters: vortex, temperature, and MLS and ACE-FTS trace gas evolution, *Atmos. Chem. Phys.*, 8, 505–522, doi:10.5194/acp-8-505-2008, 2008. 1433, 1434

10 Manney, G. L., Schwartz, M. J., Krüger, K., Santee, M. L., Pawson, S., Lee, J. N., Daffer, W. H., Fuller, R. A., and Livesey, N. J.: Aura microwave limb sounder observations of dynamics and transport during the record-breaking 2009 Arctic stratosphere major warming, *Geophys. Res. Lett.*, 36, L12815, doi:10.1029/2009GL038586, 2009. 1431, 1432, 1435

15 McInturff, R.: Stratospheric warmings: synoptic, dynamic and general-circulation aspects, NASA Reference Publ. NASA-RP-1017, NASA, Natl. Meteorol. Cent., Washington, DC, 1978. 1436

Randall, C. E., Harvey, V. L., Siskind, D. E., France, J., Bernath, P. F., Boone, C. D., and Walker, K. A.: NO<sub>x</sub> descent in the Arctic middle atmosphere in early 2009, *Geophys. Res. Lett.*, 36, L18811, doi:10.1029/2009GL039706, 2009. 1431, 1432, 1437, 1438

20 Reddmann, T., Ruhnke, R., Versick, S., and Kouker, W.: Modeling disturbed stratospheric chemistry during solar-induced NO<sub>x</sub> enhancements observed with MIPAS/ENVISAT, *J. Geophys. Res.*, 115, D00111, doi:10.1029/2009JD012569, 2010. 1432

25 Rozanov, E., Callis, L., Schlesinger, M., Yang, F., Andronova, N., and Zubov, V.: Atmospheric response to NO<sub>y</sub> source due to energetic electron precipitation, *Geophys. Res. Lett.*, 32, L14811, doi:10.1029/2005GL023041, 2005. 1431

Sander, S. P., Friedl, R. R., Golden, D. M., Kurylo, M. J., Moortgat, G. K., Keller-Rudek, H., Wine, P. H., Ravishankara, A. R., Kolb, C. E., Molina, M. J., Finlayson-Pitts, B. J., Huie, R. E., and Orkin, V. L.: Chemical kinetics and photochemical data for use in atmospheric studies, Evaluation Number 15, Publication 06-2, JPL, Pasadena, USA, 2006. 1433

30 Seppälä, A., Verronen, P. T., Clilverd, M. A., Randall, C. E., Tamminen, J., Sofieva, V., Backman, L., and Kyrölä, E.: Arctic and Antarctic polar winter NO<sub>x</sub> and energetic particle precipitation in 2002–2006, *Geophys. Res. Lett.*, 34, L12810, doi:10.1029/2007GL029733, 2007. 1431

Seppälä, A., Randall, C., Clilverd, M. A., Rozanov, E., and Rodger, C. J.: Geomagnetic activity and polar surface air temperature variability, *J. Geophys. Res.*, 114, A10312, doi:10.1029/2008JA014029, 2009. 1431

5 Siskind, D. E., Bacmeister, J. T., Summers, M. E., and Russell, III, J. M.: Two-dimensional model calculations of nitric oxide transport in the middle atmosphere and comparison with Halogen Occultation Experiment data, *J. Geophys. Res.*, 102, 3527–3546, doi:10.1029/96JD02970, 1997. 1431

10 Solomon, S., Crutzen, P. J., and Roble, R. G.: Photochemical coupling between the thermosphere and the lower atmosphere: 1. odd nitrogen from 50 to 120 km, *J. Geophys. Res.*, 87(C9), 7206–7220, 1982. 1431

Vitt, F. M., Armstrong, T. P., Cravens, T. E., Dreschhoff, A. M., Jackman, C. H., and Laird, C. M.: Computed contributions to odd nitrogen concentrations in the Earth's polar middle atmosphere by energetic charged particles, *J. Atmos. Sol.-Terr. Phys.*, 62, 669–683, 2000. 1431

15 Vogel, B., Konopka, P., Grooß, J.-U., Müller, R., Funke, B., López-Puertas, M., Reddman, T., Stiller, G., von Clarmann, T., and Riese, M.: Model simulations of stratospheric ozone loss caused by enhanced mesospheric NO<sub>x</sub> during Arctic Winter 2003/2004, *Atmos. Chem. Phys.*, 8, 5279–5293, doi:10.5194/acp-8-5279-2008, 2008. 1431, 1432

---

## Descent of odd nitrogen after sudden stratospheric warming

S.-M. Salmi et al.

---

[Title Page](#)[Abstract](#)[Introduction](#)[Conclusions](#)[References](#)[Tables](#)[Figures](#)[⏪](#)[⏩](#)[◀](#)[▶](#)[Back](#)[Close](#)[Full Screen / Esc](#)[Printer-friendly Version](#)[Interactive Discussion](#)

**Descent of odd nitrogen after sudden stratospheric warming**

S.-M. Salmi et al.

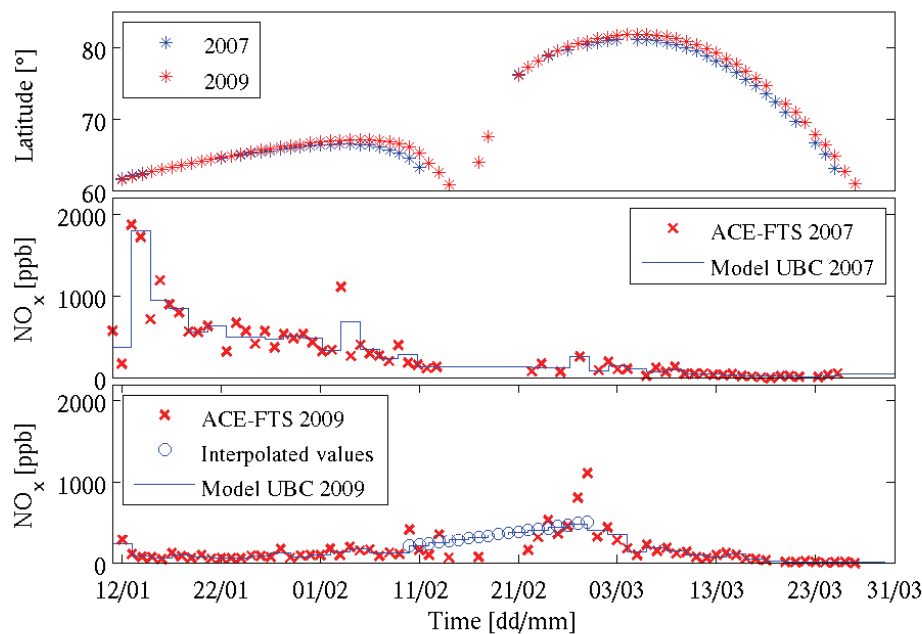


**Fig. 1.** Daily medians of ACE-FTS measurement locations north of 60° N (top) in 2007 (blue asterisk) and 2009 (red asterisk). The figure also shows mean NO<sub>x</sub> concentrations measured by ACE-FTS between 75–85 km altitudes (red crosses) and two-day means calculated from the observations (blue line) for 2007 (middle) and 2009 (bottom). Two-day means for 2009 are based on interpolated values between 10 and 28 February (blue circles).

[Title Page](#)[Abstract](#)[Introduction](#)[Conclusions](#)[References](#)[Tables](#)[Figures](#)[◀](#)[▶](#)[◀](#)[▶](#)[Back](#)[Close](#)[Full Screen / Esc](#)[Printer-friendly Version](#)[Interactive Discussion](#)

**Descent of odd nitrogen after sudden stratospheric warming**

S.-M. Salmi et al.

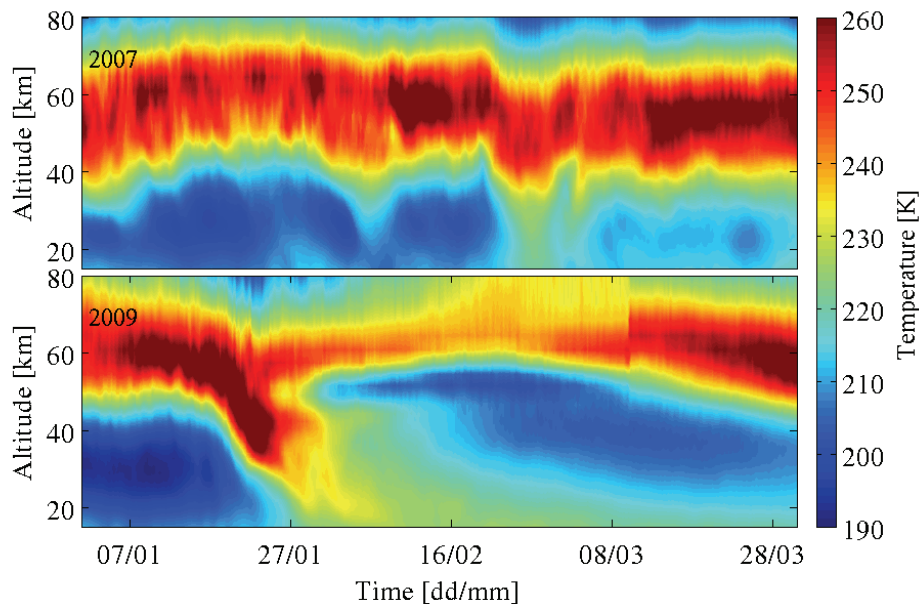


**Fig. 2.** ECMWF zonal mean temperature (K) at 75°N as a function of time and altitude for winters 2007 (top) and 2009 (bottom).

[Title Page](#)[Abstract](#)[Introduction](#)[Conclusions](#)[References](#)[Tables](#)[Figures](#)[◀](#)[▶](#)[◀](#)[▶](#)[Back](#)[Close](#)[Full Screen / Esc](#)[Printer-friendly Version](#)[Interactive Discussion](#)

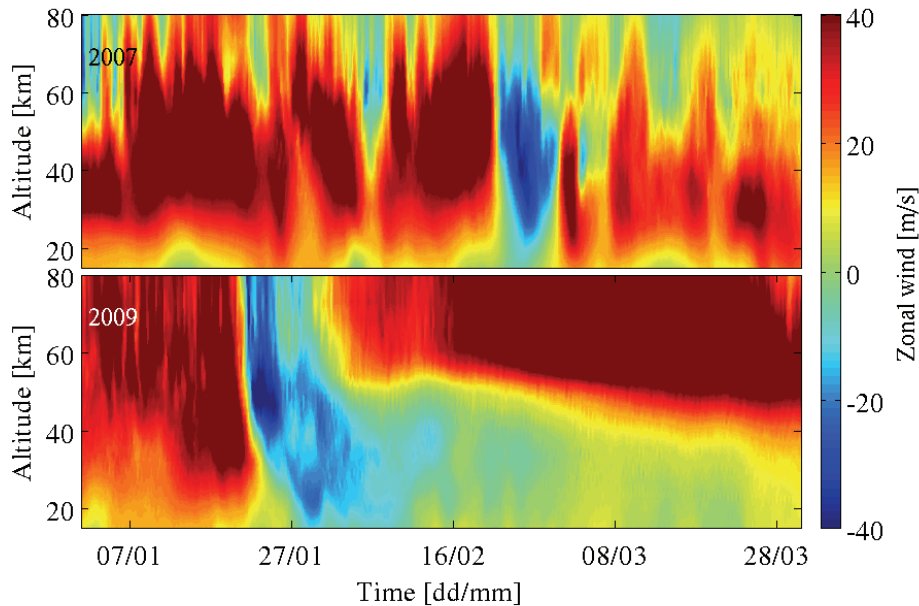


**Fig. 3.** Same as Fig. 2, but for zonal wind.

**Descent of odd nitrogen after sudden stratospheric warming**

S.-M. Salmi et al.

[Title Page](#)

[Abstract](#)   [Introduction](#)

[Conclusions](#)   [References](#)

[Tables](#)   [Figures](#)

[◀](#)   [▶](#)

[◀](#)   [▶](#)

[Back](#)   [Close](#)

[Full Screen / Esc](#)

[Printer-friendly Version](#)

[Interactive Discussion](#)



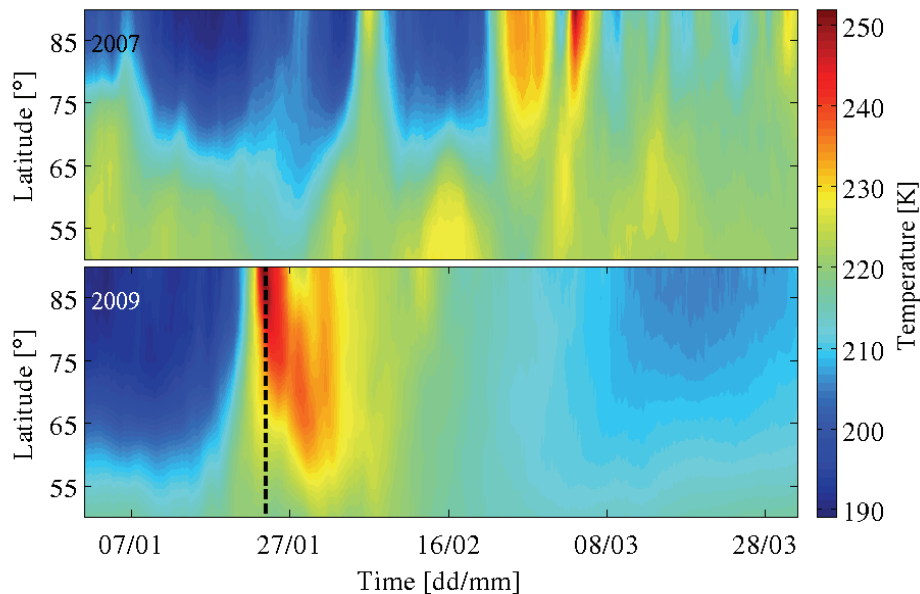


**Fig. 4.** ECMWF zonal mean temperature (K) at 10 hPa ( $\approx 30$  km) as a function of time and latitude. The upper panel represents winter 2007 and the lower one winter 2009. The vertical black dashed line in 2009 shows the date when the criteria for the major SSW were fulfilled.

**Descent of odd nitrogen after sudden stratospheric warming**

S.-M. Salmi et al.

Title Page

Abstract Introduction

Conclusions References

Tables Figures

⏪ ⏩

◀ ▶

Back Close

Full Screen / Esc

Printer-friendly Version

Interactive Discussion



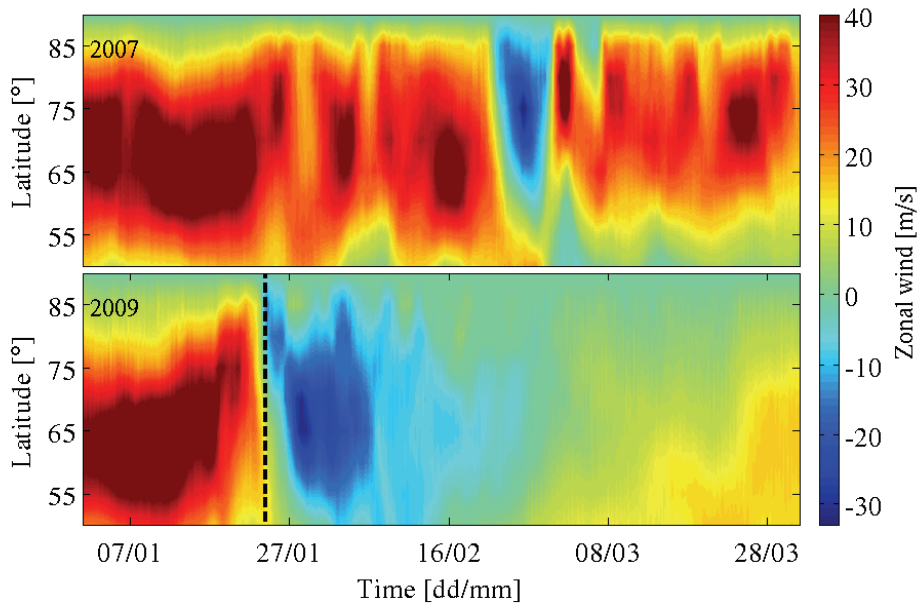


**Fig. 5.** Same as Fig. 4, but for zonal wind.

**Descent of odd nitrogen after sudden stratospheric warming**

S.-M. Salmi et al.

Title Page

Abstract Introduction

Conclusions References

Tables Figures

⏪ ⏩

◀ ▶

Back Close

Full Screen / Esc

Printer-friendly Version

Interactive Discussion



**Descent of odd nitrogen after sudden stratospheric warming**

S.-M. Salmi et al.

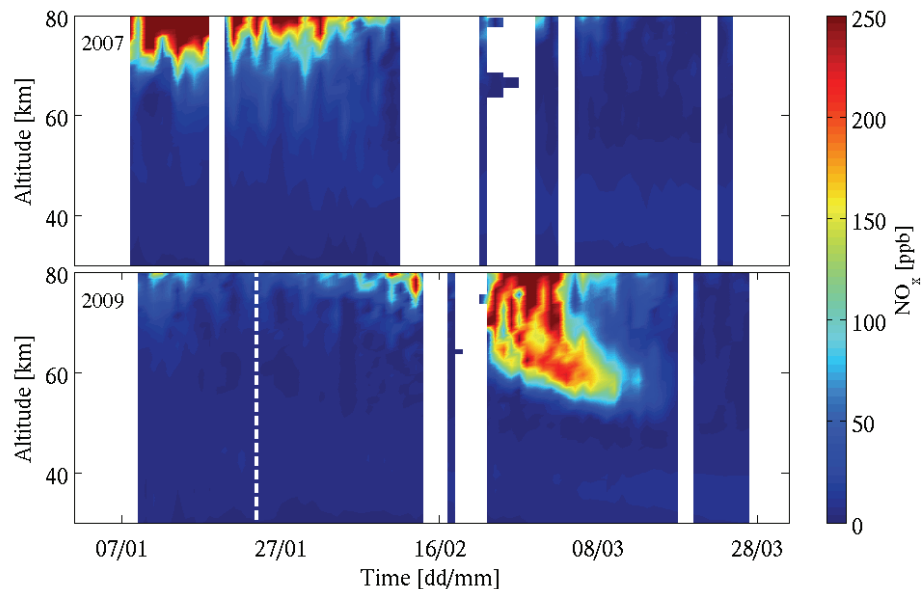


**Fig. 6.**  $\text{NO}_x$  time series (ppb) as daily medians measured by ACE-FTS. White dashed line indicates the time point, when the criteria for the major SSW were fulfilled in 2009. The upper panel is for 2007 and the lower for 2009. White regions indicate missing data or not enough data.

Title Page

Abstract

Introduction

Conclusions

References

Tables

Figures

◀

▶

◀

▶

Back

Close

Full Screen / Esc

Printer-friendly Version

Interactive Discussion

**Descent of odd nitrogen after sudden stratospheric warming**

S.-M. Salmi et al.

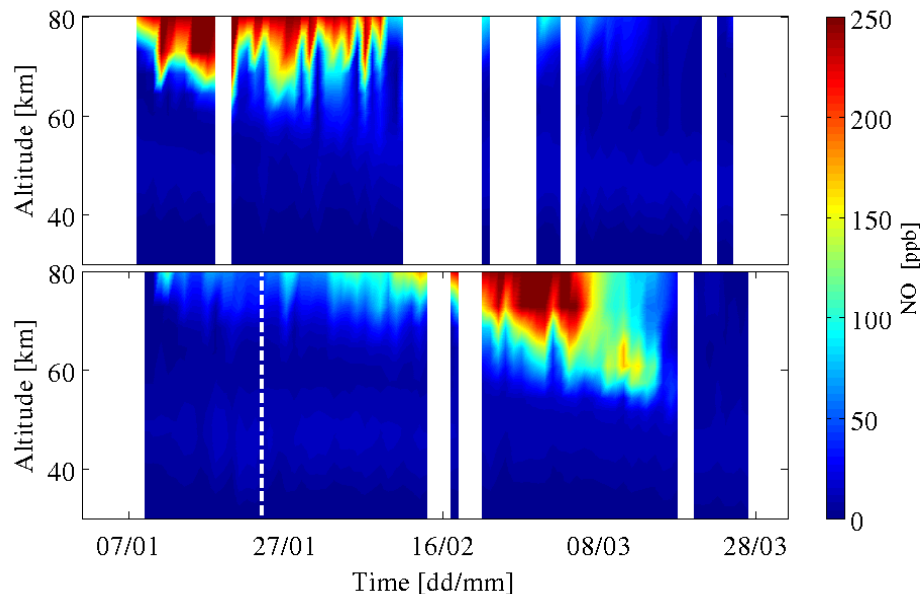


**Fig. 7.**  $\text{NO}_x$  time series (ppb) as daily means from FinROSE-CTM. White dashed line indicates the time point, when the criteria for the major SSW were fulfilled in 2009. The upper panel is for 2007 and the lower for 2009. White regions indicate missing ACE-FTS data or not enough ACE-FTS data.

[Title Page](#)[Abstract](#)[Introduction](#)[Conclusions](#)[References](#)[Tables](#)[Figures](#)[⏪](#)[⏩](#)[◀](#)[▶](#)[Back](#)[Close](#)[Full Screen / Esc](#)[Printer-friendly Version](#)[Interactive Discussion](#)

**Descent of odd nitrogen after sudden stratospheric warming**

S.-M. Salmi et al.

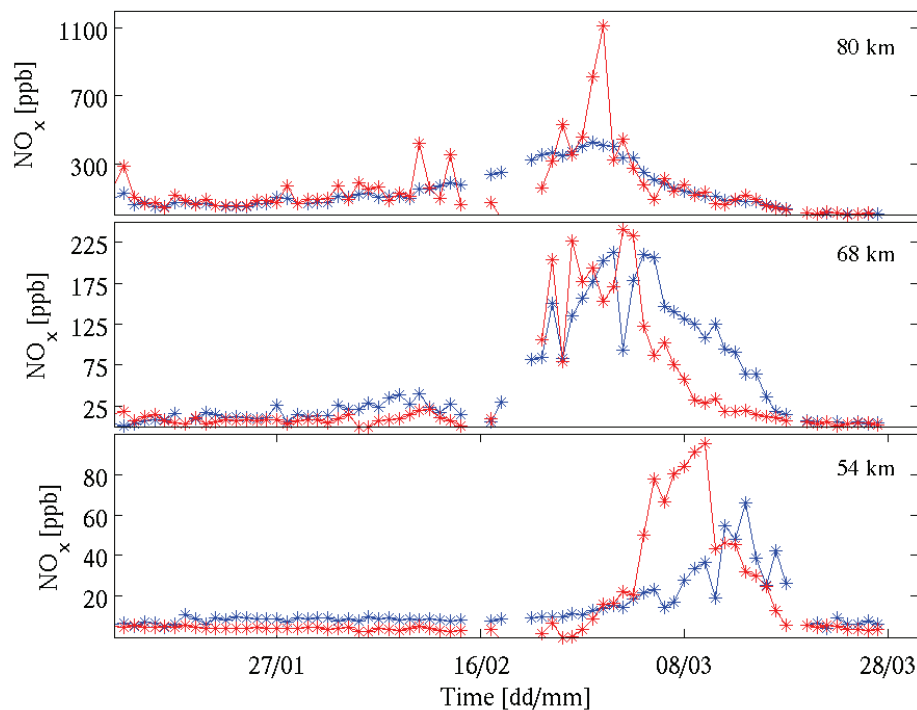


**Fig. 8.** ACE-FTS NO<sub>x</sub> observations (red line) and model results (blue line) in ppb at 80 (top), 68 (middle) and 54 km (bottom) altitudes as a function of time in 2009.

[Title Page](#)[Abstract](#)[Introduction](#)[Conclusions](#)[References](#)[Tables](#)[Figures](#)[◀](#)[▶](#)[◀](#)[▶](#)[Back](#)[Close](#)[Full Screen / Esc](#)[Printer-friendly Version](#)[Interactive Discussion](#)

**Descent of odd nitrogen after sudden stratospheric warming**

S.-M. Salmi et al.

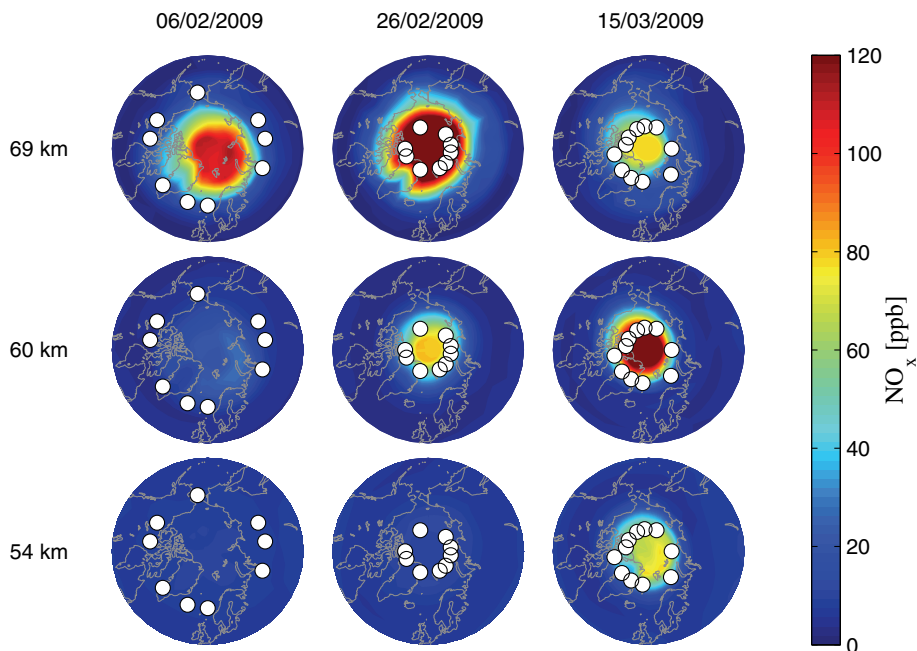


**Fig. 9.** Distribution of  $\text{NO}_x$  in ppb at 69, 60 and 51 km altitudes (rows) on 6 and 26 February and 15 March (columns) in the northern polar region ( $50^\circ\text{N}$ – $90^\circ\text{N}$ ) calculated from the model results. White circles indicate the measurement locations of ACE-FTS on that particular day.

[Title Page](#)[Abstract](#)[Introduction](#)[Conclusions](#)[References](#)[Tables](#)[Figures](#)[◀](#)[▶](#)[◀](#)[▶](#)[Back](#)[Close](#)[Full Screen / Esc](#)[Printer-friendly Version](#)[Interactive Discussion](#)

**Descent of odd nitrogen after sudden stratospheric warming**

S.-M. Salmi et al.

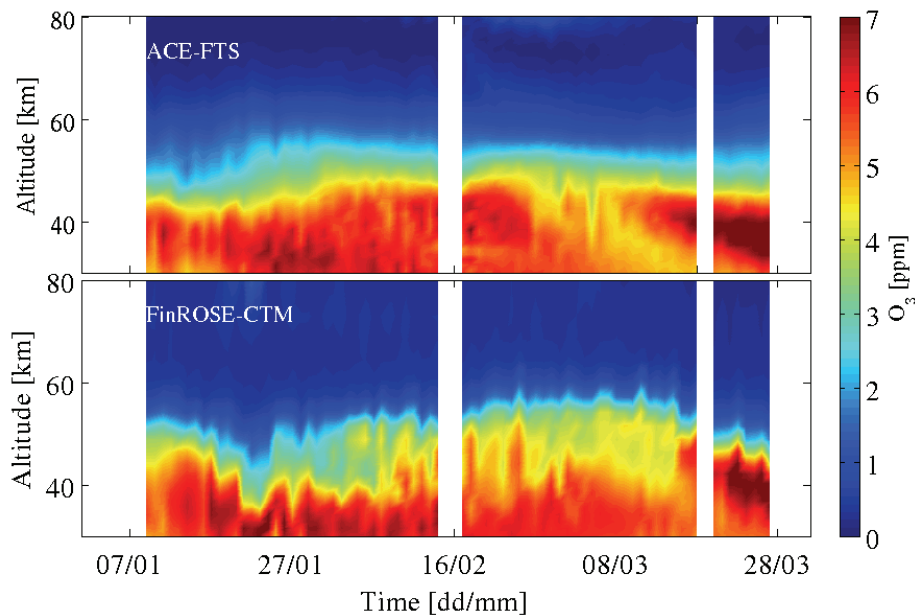


**Fig. 10.** ACE-FTS (top) and FinROSE-CTM (bottom) ozone time series in ppm as a function of altitude for early 2009 in ACE-FTS measurement locations.

[Title Page](#)[Abstract](#)[Introduction](#)[Conclusions](#)[References](#)[Tables](#)[Figures](#)[⏪](#)[⏩](#)[◀](#)[▶](#)[Back](#)[Close](#)[Full Screen / Esc](#)[Printer-friendly Version](#)[Interactive Discussion](#)